Title

Tree growth decline to warm-wet conditions in boreal forests is linked to stand density

Authors

Zhao, Bingqian

Zhu, Yihong

Gao, Lushuang

et al.

Publication Date

2024-10-01

DOI

10.1016/j.fecs.2024.100266

Forest Ecosystems 12 (2025) 100266

Contents lists available at ScienceDirect

Forest Ecosystems

journal homepage: www.keaipublishing.com/cn/journals/forest-ecosystems

Tree growth decline to warm-wet conditions in boreal forests is linked to stand density

Bingqian Zhao [a,b], Yihong Zhu [c], Lushuang Gao [a,b,*], Qibing Zhang [d], Mingqian Liu [a,b,e], Klaus von Gadow [f,g]

[a] Research Center of Forest Management Engineering of State Forestry and Grassland Administration, Beijing Forestry University, Beijing, 100083, China
[b] State Forestry and Grassland Administration Key Laboratory of Forest Resources & Environmental Management, Beijing Forestry University, Beijing, 100083, China
[c] Department of Environmental Science, Policy and Management, University of California, Berkeley, 94704, USA
[d] State Key Laboratory of Vegetation and Environmental Change, Institute of Botany, Chinese Academy of Sciences, Beijing, 100093, China
[e] Laboratory of Wood Technology, Ghent University, Coupure links 653, 9000, Ghent, Belgium
[f] Faculty of Forestry and Forest Ecology, Georg-August-University Göttingen, Büsgenweg 5, D-37077, Göttingen, Germany
[g] Department of Forestry and Wood Science, Faculty of AgriSciences, Stellenbosch University, Stellenbosch Private Bag X1, Stellenbosch, 7602, South Africa

ARTICLE INFO

Keywords:
Growth decline
Stand density
The southern edge of boreal forests
Larix gmelinii

ABSTRACT

Warm-wet climatic conditions are widely regarded as conducive to remarkable tree growth, alleviating climatic pressures. However, the notable decline in tree growth observed in the southern edge of boreal forests has heightened concerns over the spatial-temporal dynamics of forest decline. Currently, attaining a comprehensive grasp of the underlying patterns and their propelling factors remains a formidable challenge. We collected tree ring samples from a network of 50 sites across the Greater Xing'an Mountains. These samples were subsequently grouped into two distinct clusters, designated as Groups A and B. The percentage change of growth (GC, %) and the proportion of declining sites were utilized to assess forest decline. The decline in tree growth within *Larix gmelinii* forests exhibits significant regional variation, accompanied by temporal fluctuations even within a given region. Group A exhibited a pronounced increase in frequency (59.26%) of occurrences and encountered more severe declines (21.65%) in tree growth subsequent to the 1990s, contrasting sharply with Group B, which observed lower frequencies (20.00%) and relatively less severe declines (21.02%) prior to the 1980s. The primary impetus underlying the opposite radial growth increments observed in *Larix gmelinii* trees from the interplay between their differential response to temperatures and wetter climatic conditions, which is significantly influenced by varying stand densities. In cold-dry conditions, low-density forests may experience soil water freezing, exacerbating drought conditions and thereby inhibiting tree growth, in Group B. Trees growth in high-density stands is restrained by warm-wet conditions, in Group A. These results provide new insights into the variability at the southern edge of the boreal forest biome with different responses to density and climate.

1. Introduction

Understanding how climate change affects boreal forests across spatial-temporal scales is crucial for anticipating its impacts on terrestrial ecosystems. The rising temperatures, decreased precipitation, and occurrence of extreme weather events have been influencing the diversity and composition of forests (Lloyd and Bunn, 2007). Such forest decline has often led to reduced tree growth decline and even mortality (de Castillo et al., 2022a). While there is increasing attention to the impact of climate change on forest decline in boreal forests (Liu et al., 2013; Gauthier et al., 2015; Li et al., 2023), there is a lack of research on a large spatial scale and long-time scale of boreal forests, as well as the drivers causing declines, especially at the southern edge of the taiga.

Forest decline under climate change has been widely detected by studies at various scales (Allen et al., 2010; Zhou et al., 2020; Hernández-Alonso et al., 2023). Evidences of decline patterns was presented through the analysis of 229 tree-ring width chronologies from nine regions across three continents in the Northern Hemisphere, revealing regional variations in decline periods (Liu et al., 2022). In European beech forests, future rising temperatures could lead to a widespread

* Corresponding author. Research Center of Forest Management Engineering of State Forestry and Grassland Administration, Beijing Forestry University, Beijing, 100083, China.
E-mail address: gaolushuang@bjfu.edu.cn (L. Gao).

https://doi.org/10.1016/j.fecs.2024.100266
Received 9 August 2024; Received in revised form 9 October 2024; Accepted 23 October 2024

decline of 20%–40% in beech growth (Martinez del Castillo et al., 2022). Since the 1940s, there has been an observed increase in the proportion of the circumpolar boreal forests exhibiting negative responses to warmer temperatures (Lloyd and Bunn, 2007). The decline of *Abies alba* across different generations in Central Europe commenced after 1960 (Podlaski, 2021).

The findings of certain studies suggest that adequate water-heat conditions can alleviate energy deficiency, which arises from insufficient thermal energy and moisture in trees for vital processes like photosynthesis and respiration, thereby facilitating tree growth (Bai et al., 2019). Other research indicates that water scarcity restricts tree growth, with trees exhibiting a positive response to increased precipitation (Chen et al., 2012; Yu et al., 2018; Zheng et al., 2022a, 2022b). In contrast, in regions experiencing temperature increases and precipitation decreases, drought inhibits tree growth, thereby posing threats of decline and mortality to boreal forests (Liu et al., 2013). However, observations of radial growth records in these regions under warmer and wetter conditions present variable results.

Moreover, climate-growth responses of boreal forests exhibit regional variations (Lloyd and Bunn, 2007; Sánchez-Salguero et al., 2017; Camarero et al., 2018; Li et al., 2020). The variability of tree growth responses to climate is influenced by factors such as tree age (Liu et al., 2013), topography (Bai et al., 2019), and stand structure (Cao et al., 2021). The variations in climatic limiting factors, both spatially and temporally, account for the disparities observed in tree growth response along latitudinal and elevational gradients (Bai et al., 2019; Yasmeen et al., 2019). The baseline of the larch populations exhibiting negative growth-temperature responses decreased with latitude and elevation, based on radial growth series across Eurasian boreal larch forests (Li et al., 2023). During drought periods, high-density young forests exhibit greater drought resistance than low-density old forests, as trees in dense forests regulate stomata to reduce water loss and prevent hydraulic failure, enabling better growth in young forests (Zhang et al., 2022a, 2022b). Forest density can control the sensitivity of radial growth of trees to climate fluctuations. January precipitation and temperature inhibit the growth of dense forests, while July precipitation and temperature promote the growth of dense forests (Kholdaenko et al., 2022). Given the wide range of latitudes and longitudes in the study area, leads us to hypothesize there are variations in forest growth responses to climate and density, with temperature exerting a relatively higher contribution.

Despite the extensive distribution and significant ecological relevance of boreal forests, the southern edge of the boreal forest biome has received relatively limited attention. Forest ecosystems of the Greater Xing'an Mountains in northern China serve as a representative of example the southern edge of the boreal forest biome (Liu et al., 2023). This region plays a crucial role in the terrestrial carbon cycle (Yang et al., 2023). *Larix gmelinii*, as the dominant tree species in the region (Yasmeen et al., 2019), has sparked controversy regarding its response to climate in the Greater Xing'an Mountains. The growth of young stands currently located in less suitable areas was found to improve under changing climatic conditions (Pang and Zhao, 2023). The growth decline observed at low elevations (Bai et al., 2019), contrasts with the absence of decline in larch forests located in the north of the Greater Xing'an Mountains (Zhang, 2022). These inconsistencies may be attributed to spatial and temporal variations in growth response to climatic limiting factors (Lloyd and Bunn, 2007).

In this study, we analyzed the tree radial growth and diverse climate data on 50 permanent observational sites in southern edge of boreal forests. We investigated both the radial growth patterns and the potential climatic and stand structural driving factors within a large region and a long time scale. Specifically, we hypothesize that,

(i) There are particular temporal patterns of climate-induced boreal forest decline, the patterns differ by timing, frequency, and intensity.

(ii) The spatial pattern of climate-induced forest decline is linked to stand density. As the climate becomes warmer and wetter, dense forests are particularly susceptible to its impact (Fig. 1).

2. Materials and methods

2.1. Study area

The study area (47°32′–53°22′ N, 120°03′–126°30′ E) is located in the Greater Xing'an Mountains, located in the northwest of Heilongjiang Province and the northeast of the Inner Mongolia Autonomous Region, China (Fig. 2). The region exhibits a cool temperate continental climate that is influenced by the East Asian monsoon. The annual average temperature is −2.8 °C. The frost-free period spans from 90 to 110 days, and the average annual precipitation amounts to 746 mm. The extreme minimum temperature of −52.3 °C occurred on February 13, 1969, while the extreme maximum temperature of 37.0 °C was recorded on June 29, 2010. The predominant forest soil types in the study area consist mainly of brown coniferous forest soils and dark brown soils (Wang et al., 2001). The forest types are primarily larch forests and mixed larch forests. The dominant tree species is *Larix gmelinii*, in mixtures with secondary three species: *Betula platyphylla*, *Quercus mongolica*, and *Populus davidiana* (Wang et al., 2020). In July 2017, we established 50 permanent circular plots with a radius of 17.85 m. For each plot, we recorded the species, DBH, tree height (H) and coordinates of all trees with a diameter at breast height (DBH) $\geq$ 5 cm, as well as the soil depth, elevation and slope.

2.2. Tree-ring data

In July 2017, we conducted a meticulous sampling campaign by extracting a core with a precise diameter of 5.15 mm at breast height from each eligible tree across all designated sites. Ensuring the integrity of our samples, we excluded trees exhibiting curved stems, extensive heart rot, stem abrasion, or fungal infections. Following the sampling process, we took precautionary measures by filling the sampling holes with petroleum jelly to safeguard against potential infestations by pests or diseases. The tree cores were placed inside straws of uniform size to prevent any potential damage, and each straw was labeled straw with a tag indicating the sample number and tree species. In the laboratory, we carefully placed the cores in a cool and well-ventilated environment to facilitate their natural air-drying process. Once thoroughly dried, we meticulously affixed each core to a suitable wooden trough using white glue, further securing them with tape to prevent any warping and ensuring that the wood fibers maintained a perpendicular alignment with the trough. To maintain comprehensive documentation, we meticulously recorded the tree number, diameter at breast height (DBH), species, fixation time, and any other pertinent details. After ensuring that the glue had thoroughly dried, we embarked on a polishing process utilizing a sanding machine equipped with six varying grades of sandpaper, ranging from a coarse 100 grit to a fine 1500 grit. This extensive sanding ensured a smooth and luminous surface, facilitating the clear examination of wood structure and the distinct delineation of tree-ring boundaries. Following the processing of the tree cores, we painstakingly marked the annual ring boundaries, facilitating the precise measurement of annual ring widths and facilitating the crucial cross-dating process.

We used the TSAP-Win program and the LinTab 5 tree ring measuring device (Frank Rinntech Company, Heidelberg, Germany) with a measurement accuracy of 0.001 mm to process the core widths. The COFECHA program was used to conduct correlation analysis on the sample sequences, aiming to identify and eliminate any anomalous radial growth or measurement errors. After rigorous scrutiny, we excluded those cores that demonstrated poor correlation with the master sequence and posed difficulties in cross-dating, ensuring the integrity of our data set. Consequently, we retained an impeccable selection of 1400 tree cores, characterized by high correlation values and clearly discernible annual rings, providing a robust foundation for our subsequent analysis. With

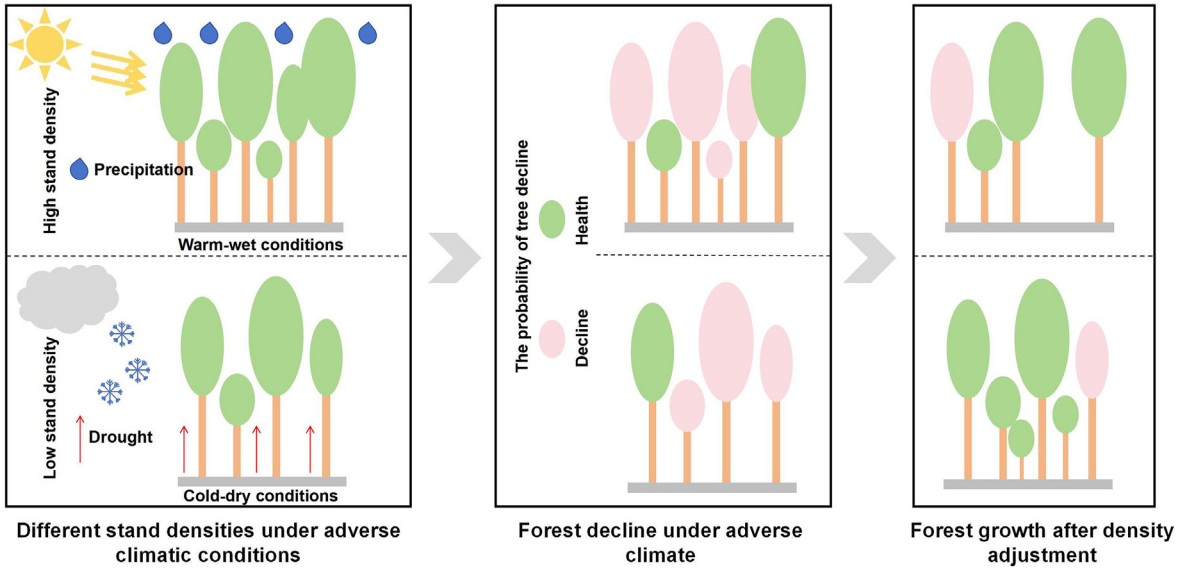

Fig. 1. Diagram explaining hypothesis 2.

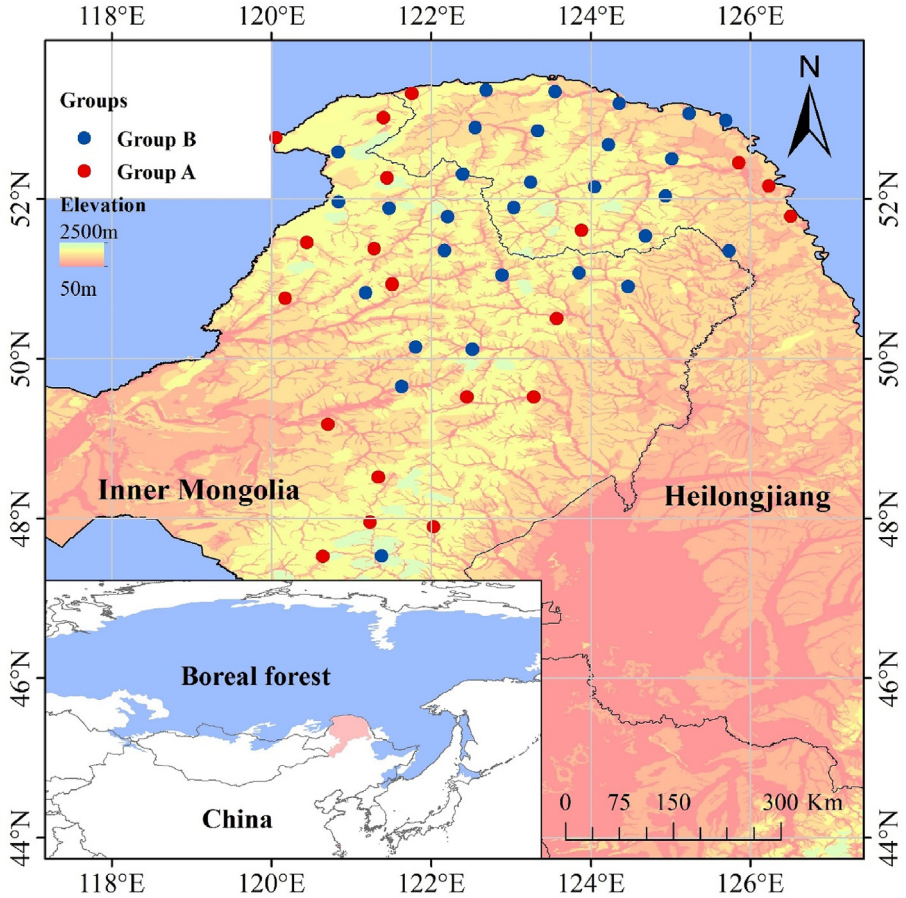

Fig. 2. Map of the study area showing the 50 plots locations. The method of plot grouping is described in section 2.4.1. Group A is represented by the red points, while Group B is represented by the blue points, with a total of 21 and 29 plots respectively. (For interpretation of the references to color in this figure legend, the reader is referred to the Web version of this article.)

the advantage of providing inter-annual radial growth of trees over a long temporal scale (Fritts, 1966), tree ring networks are widely used to quantify forest decline. To remove the age-related trend, we applied spline functions with a step size of 60 years to detrend each tree-ring series (R *dplR* package). Finally, we used the ARSTAN software to establish standardized chronologies for each site. From 1830 to 2016, the minimum number of cores was 5, indicating satisfactory chronology quality for analysis during this period. All 50 chronologies exhibited

expressed population signals (EPS) > 0.85 during 1901–2016, indicating that the quality of the chronologies for this period was suitable for subsequent analyses of growth responses to climate.

2.3. Climate data

The climate data for each month were obtained from ClimateAP for the period 1901–2016 (Wang et al., 2017), with a 4 km × 4 km spatial resolution. The data were obtained from Parameter-elevation Relationships on the Independent Slopes Model (Daly et al., 2008) and the WorldClim database (Hijmans et al., 2005). We selected the monthly average temperature and precipitation values (Table 1) from June to August as indicators of the pivotal growing season for trees in this region. These months encompass climatic conditions, including temperature and precipitation, that are highly conducive to growth, rendering this time frame crucial for analyzing the relationship between climate factors and tree growth performance.

2.4. Statistical analyses

2.4.1. Hierarchical clustering

We used the R package *scatterpie* with the *ward.D2* method and combed the inter-correlation of tree-ring width chronologies from each site to divide the 50 sites into two Groups A and B. This method, known as hierarchical clustering, was employed to cluster sites based on radial growth. The distribution of Groups A and B is illustrated in Fig. 2. The clustering involved iteratively merging or splitting data points to create a hierarchical tree structure with an aim to reveal the intrinsic relationships and similarities among the 50 sites (Murtagh and Legendre, 2014).

2.4.2. Determination of decline

To quantify the occurrence time, frequency, and intensity of declining radial growth, we calculated the proportion of declining sites and the percentage change of growth (GC, %) annually. A year was considered to have experienced decline in a group if the proportion of declined sites >20% and the declined GC significantly exceeded the increase in GC. We identified decline by comparing the annual ring width of each site to the average annual ring width of its respective group. We used the mean value method to calculate GC (%) (Nowacki and Abrams, 1997):

$$GC = \frac{M_2 - M_1}{M_1} \times 100\%$$

where M_1 and M_2 represent the mean of the tree ring widths for the preceding 5 years and the subsequent 5 years, respectively. For example, M_2 and M_1 were the mean tree ring widths for the periods 2012–2016 and 2007–2011, respectively, which were used to calculate GC in 2011. Subsequently, we employed this approach to calculate GC of each tree in Groups A and B:

GC > 0 indicates the increasing, GC < 0 the declining extent in tree radial growth. We refer to the mean of the positive GC as *the increasing extent*, and the mean of the negative GC as *the declining extent* in each year.

We observe three types of growth decline. When the proportion of declining plots within a given period exceeds 20% and the declining extent surpasses the increasing extent, we refer to this period as *a period of multifaceted decline*. When the proportion of declining plots exceeds 20%, we refer to this period as a period of *unilateral proportional decline*. When the declining extent surpasses the increasing extent, we refer to this result as the *extent of unilateral decline*.

Table 1
Explanation of climate variables.

Type	Abbreviation	Explanation	Unit
Temperature	LT	Low temperature	°C
	HT	High temperature	°C
	DD > 5	Degree-days above 5 °C, growing degree-days	–
	NFFD	The number of frost-free days	–
Precipitation	P	Precipitation	mm
	CMD	Hargreaves climatic moisture deficit	–

2.4.3. Quantify forest stand density

Stand density is not only a crucial indicator of stand growth, but also a significant controllable factor in artificial forestry practices. Reineke (1993) introduced what is perhaps the most comprehensive formulation of the stand density index (SDI) equation:

$$SDI = N\left(\frac{D_0}{D}\right)^b \quad (2)$$

where N represents the number of trees per hectare in the real stand, D_0 is the standard average diameter, and D is the average diameter of the real stand. Using this equation, we calculated the SDI for various sites.

2.4.4. Metrics to measure growth-climate correlations

We conducted principal component analysis (PCA) on the correlations between the tree ring width index (RWI) and temperature and precipitation for 50 sites spanning from 1901 to 2016 (Wang et al., 2022), aiming to enhance our understanding of the RWI-climate relationship at each site. We extracted the scores of each site on the PCA axis, which represented the magnitude of the correlation between RWI and climate. Additionally, we extracted the weights of each climate indicator on the PCA axis, indicating their respective influences on the RWI - climate correlation. We performed the calculations using R 4.2.3 and created figures using the software Origin 2022.

3. Results

3.1. Temporal and spatial patterns of declining tree growth

We applied a hierarchical clustering approach to segregate the 50 sites into two distinct groups, namely Group A (encompassing 21 sites) and Group B (comprising 29 sites, Fig. 2). Group A exhibited a pronounced pattern, with a higher frequency of decline events (59.26%) and more severe declines (21.65%) manifesting post-1990 (Fig. 3a, b, c). Conversely, Group B displayed a different trend, experiencing a lower frequency (20.00%) of decline events but with less severity (21.02%) during the period from 1960 to 1980 (Fig. 3d, e, f). Prior to 1970, Group A encountered four decline events, albeit with relatively low frequencies. Similarly, Group B witnessed three decline events post-2000, also marked by low frequencies of occurrence. In addition, the proportion of declining sites and the severity of decline events reflected through the RWI further quantify the characteristics of decline events. In 1966, 1968, 1973, 1986, 1987, 1991, 1993, 2000 and 2008, Group A experienced unilateral decline in proportion (Fig. 3b and c). In 1942, Group A experienced unilateral decline in extent (Fig. 3b and c). In 1972, 1975, 1979, 1986, 1987 and 1992, Group B experienced unilateral decline in proportion (Fig. 3e and f). In 1911, 1914, 1919, 1921, 1954, 1970 and 2014, Group B experienced unilateral decline in extent (Fig. 3e and f).

3.2. Drivers of tree growth decline

The principal components analysis (PCA) revealed that PC1 and PC2 accounted for 81.48% and 16.90% of the total variation, respectively. It is evident that both temperature and precipitation act as pivotal factors, collectively influencing the intricate relationship between growth-climate (Fig. 4). Based on the scores of each climate indicator, Groups A and B exhibited distinct responses primarily in terms of their correlations with RWI and low temperature (LT), as well as precipitation (P). Specifically, Group A displayed a negative response to both LT and P, while Group B demonstrated a positive response to LT. The differential climatic responses observed between Groups A and B were significantly

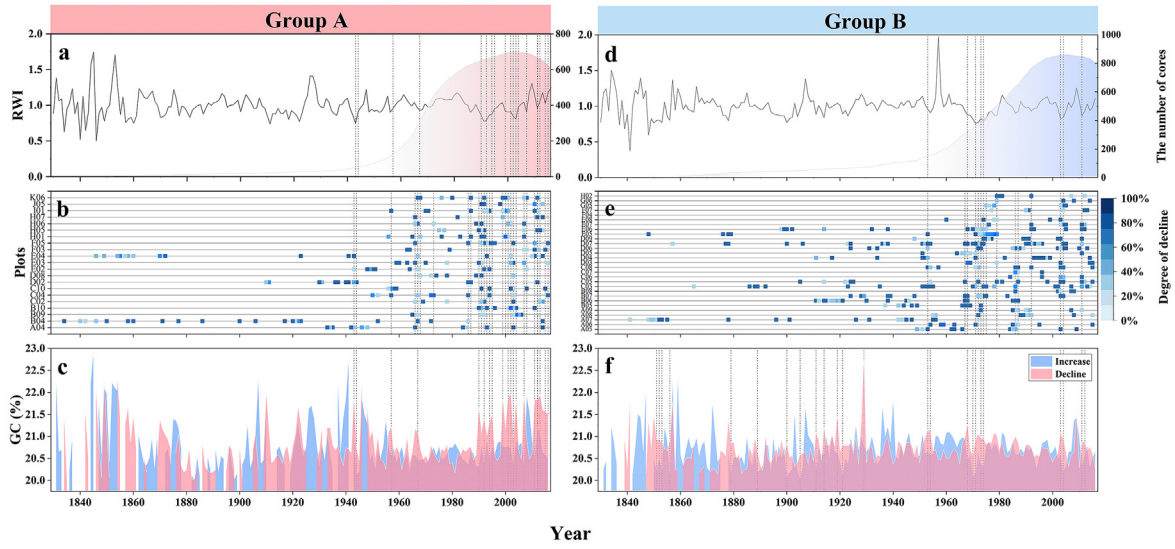

Fig. 3. The timing, frequency, and intensity of decline events in two groups from 1830 to 2016. **a, d**: RWI of Groups A and B. The dashed lines in **a** represent the years of decline, and refer to the common years identified in **b** and **c**. The dashed lines in **d** indicate the common years identified in **e** and **f**. The shaded area represented the number of cores. **b, e:** The vertical axis represents the different sites in Groups A and B, while the points on each row represent the decline events that occurred in those sites between 1830 and 2016. The intensity of the color at each point represents the severity of the decline events, darker colors indicate more severe declines. **c, f:** Increased and declined GC in Groups A and B. In order to compare the magnitudes of declined and increased GC in the graph, we converted the negative values of declined GC into positive values. (For interpretation of the references to color in this figure legend, the reader is referred to the Web version of this article.)

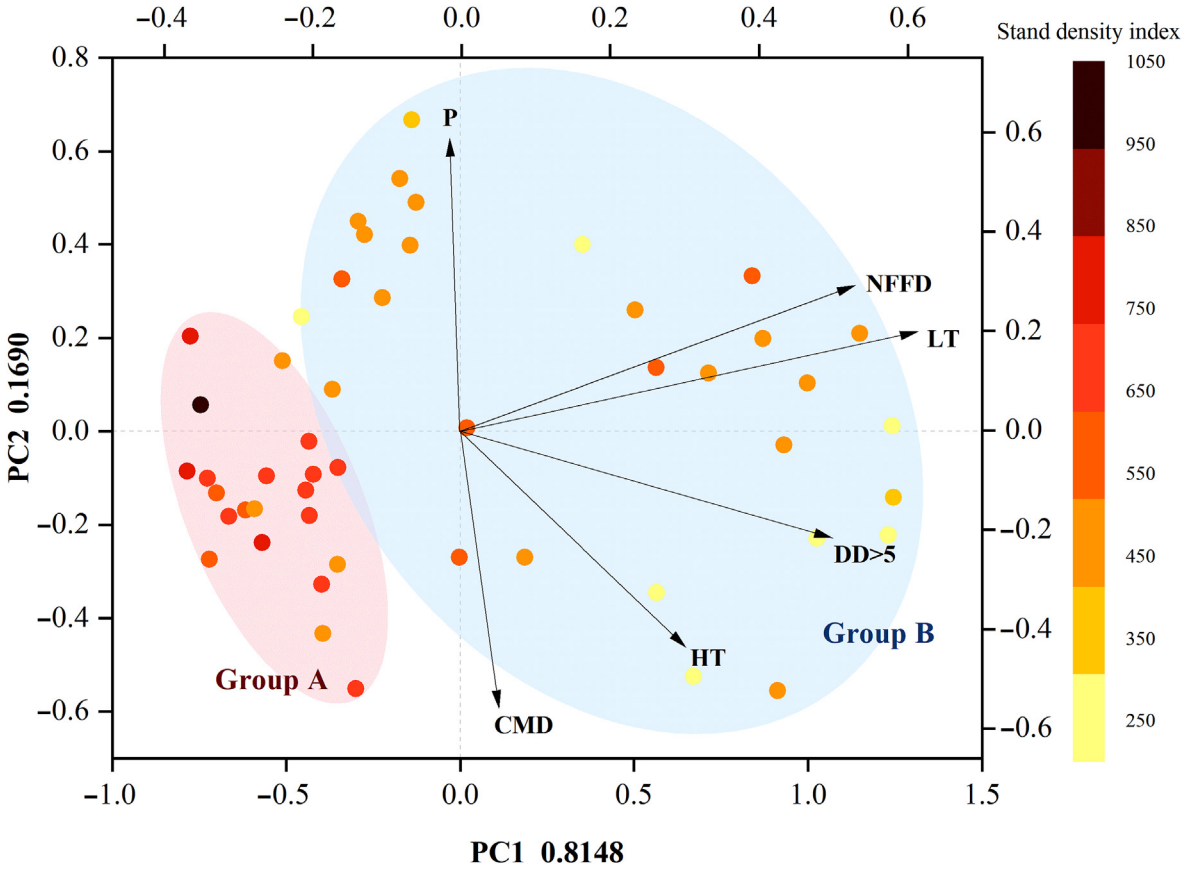

Fig. 4. Principal component analysis (PCA) for the correlations of RWI with degree-days above 5 °C (DD > 5), the number of frost-free days (NFFD), high temperature (HT), growing season low temperature (LT), Hargreaves climatic moisture deficit (CMD) growing season precipitation (P) (each climate indicator was averaged from June to August of the current year) for the 50 sites. The *X* and *Y* axes represented the correlations between the RWI of each site and various climate indicators, while the color of each point represented the SDI of 50 sites. (For interpretation of the references to color in this figure legend, the reader is referred to the Web version of this article.)

associated with SDI. As SDI increased, the promoting effects of LT and P on tree growth gradually decreased, and could even become negative (Fig. 5). When SDI <551, both LT and P promoted tree growth. When 551 < SDI <680, LT inhibited growth while P promoted growth. When SDI >680, both LT and P caused a reduction in tree growth. The SDI of Group A exhibited a significantly higher value compared to that of Group B ($P < 0.05$). Group B demonstrated a negative growth response to P, whereas Group A displayed a positive growth response to P.

4. Discussion

4.1. The effects of temperature and precipitation on the growth of Larix gmelinii varied at different stand densities

The stand density of individual sites serves as a pivotal factor in determining the differential effects of temperature and precipitation on the radial growth of *Larix gmelinii* (Fig. 5). Forest decline, in turn, serves as a tangible manifestation of the impact of climate change on tree growth (Figs. 4 and 6). Our analysis reveals a significant correlation between temperature and precipitation during the growing season and forest growth decline (Figs. 4 and 6), with variations observed across different stand densities (Fig. 5). One study revealed that forest growth can be influenced by spatial varying topographic and microclimatic conditions (Pang and Zhao, 2023). Interestingly, Cao et al. (2021) proposed that a potential relationship between stand density and climate sensitivity, suggesting that low-density stands exhibit a stronger negative correlation with temperature while high-density stands exhibit a stronger negative correlation with precipitation. The conjunction of these two discoveries provides a compelling rationale. Forests characterized by high stand density (Group A) was observed to growth decline under elevated temperatures and humidity. In contrast, forests characterized by lower stand density (Group B) experience decline in response to colder and drier environments (Fig. 6). The influence of climate on forest decline is evidently discernible, with stand density playing a crucial role in regulating the response to climatic factors (Fig. 5). This obtained result validates our initial anticipation that dense forests are particularly susceptible to the impact of warm and humid conditions. Furthermore, our observations revealed that colder and drier climatic conditions lead to a marked decline in growth, particularly prevalent in sparse forests (Figs. 4 and 6). This observed phenomenon can likely be attributed to the combined effects of low temperatures that freeze soil moisture and existing drought, rendering trees more vulnerable to frost damage and drought stress (Zhang et al., 2023). Conversely, in high-density stands, the trees exhibit resilience against such cold, dry conditions. The dense canopy effectively mitigates wind exposure and enhances soil moisture retention by minimizing evaporation (Zhang et al., 2022a, 2022b). Furthermore, the collective presence of these trees fosters a microclimate that tempers extreme temperature fluctuations (De Mello et al., 2024), thereby mitigating the threat of frost damage. By providing mutual protection, they potentially alleviate the detrimental impacts of adverse weather conditions on individual tree growth.

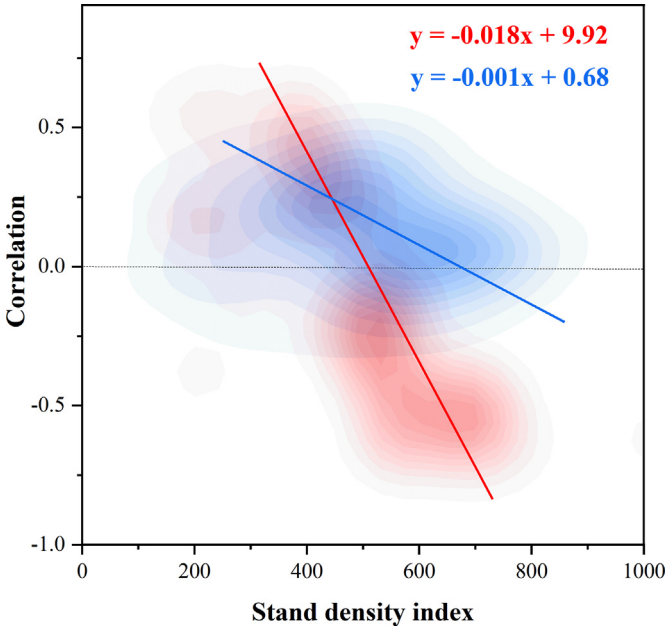

Fig. 5. The response of growth to LT and P at different stand densities. The red and blue *Y* values represented the correlations of growth with LT and P, respectively, among the 50 sites. The straight lines were obtained from linear regression. (For interpretation of the references to color in this figure legend, the reader is referred to the Web version of this article.)

The previous studies provide evidence that in boreal forests, the combination of sufficient precipitation and elevated temperatures can effectively prolong the growing season, and thereby facilitating tree growth (Gao et al., 2022). However, during recent decades of rapid warming, noticeable declines in growth have been observed in some larch forests located at the southern edge of the boreal forest biome (Fig. 3). This may be due to the fact that in high-density forests, water and nutrient resources may still be insufficient to support the growth of all trees, even in warm and wet climates. The density of tree population results in reduced access to light, water and nutrients for each individual tree (Collet et al., 2014). Due to the density, shading is evident in the understory, leading to a build-up of moisture in the soil (Wei and Liang, 2021). Simultaneously, the moist climate further amplifies the soil moisture content. This excessive soil water content diminishes respiratory efficiency within the tree root system, leading to root hypoxia (Zheng et al., 2022a, 2022b). Moreover, densely packed trees are more likely to spread pests and pathogens, especially in a humid climate, which can seriously affect tree health and growth (Jia et al., 2020). In summary, under warmer and wetter climatic conditions, tree growth is impeded in high-density forests due to increased resource competition, root hypoxia and the pests and diseases spread. This aforementioned pattern implies that although a warm and wet climate may favor the growth of certain boreal forests, there can be adverse effects on high-density in certain cases, leading to forest decline. Forest management strategies should be adapted to local climatic conditions and stand density dynamics in order to mitigate forest decline. In high-density forests, where competition for resources can render trees more susceptible to stress during warm and wet conditions, selective thinning can improve forest health by reducing competition and enhancing resilience against disease. Previous studies support this approach, showing that thinning increases air circulation and resource availability, thereby contributing to a reduction in mortality rates. Conversely, it is worth noting that increasing stand density may prove advantageous for low-density forests situated in colder and drier environments. A denser canopy can improve microclimatic conditions, such as moisture retention and temperature moderation, thereby promoting tree survival and productivity. This adaptive management approach, which involves adjusting density based on specific environmental pressures, can optimize forest health and productivity, thus increasing the resilience of forests to future climatic changes.

4.2. The temporal and spatial variation of growth decline at the southern edge of the boreal forest biome is affected by differences in the growth-climate relationship

In an effort to elucidate the detrimental impacts of climate change on forest growth, researchers often translate forest decline into quantifiable metrics, offering a clearer understanding of its scope. Compared to preceding investigations, our study adopted an array of indicators, enabling us to meticulously quantify not only the timing and duration but also the severity of forest decline, as manifested through radial tree growth. This

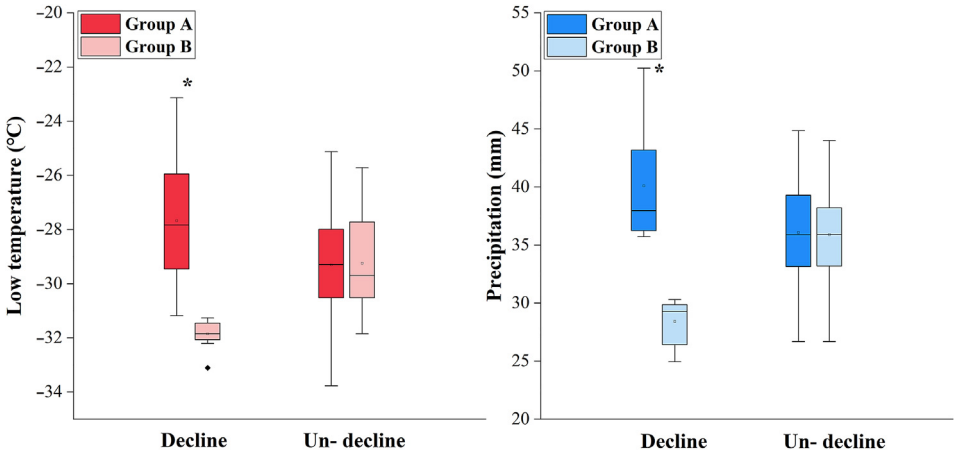

Fig. 6. The difference in low temperatures and precipitation between the period of decline and un-decline for Groups A and B.

comprehensive approach ensures a more nuanced and accurate portrayal of the complex effects of climate change on forest health. Podlaski (2021) used tree ring width as an indicator to measure the decline of *Abies alba* growth in Europe. Basal area increment (BAI) serves as another indicator employed to estimate decline in European beech forests between 1955 and 2016 (Martinez del Castillo et al., 2022). However, both studies solely relied on a single indicator to quantify forest decline, and the lack of an accurate identification of the decline may lead to erroneous conclusions. It is crucial to accurately identify the extent of decline by considering the proportion of declining plots, which indicates both the declining and increasing plots within a given area. The percentage change of growth (GC) serves as a valuable indicator, reflecting the overall trends of increase and decrease in tree radial growth within a given area. To ensure a robust assessment of forest decline, we have selected two indicators: GC, and the proportion of declining sites. This fortifies our analysis, providing a more comprehensive and reliable evaluation of the extent and severity of forest decline.

As expected, the observed decline exhibits significant variation across diverse regions and, within a given region, demonstrates temporal fluctuations over time. Post-1990s, Group A experienced higher frequencies (59.26%) and more severe declines (21.65%). Between 1960 and 1980, Group B encountered lower frequencies (20.00%) and less severity (21.02%). A study pinpointed 1963–1966 as the period of decline for larch forests in Genhe (Zhang, 2022), and our research findings, concerning the decline phases observed in Group B, are in close accordance with these previously reported observations. However, the decline characteristics of forests in Group A differ significantly from those reported in previous studies. This disparity may stem from the narrower geographical scope of the earlier research. Consequently, it is imperative to consider geographical scales when investigating the impacts of climate change on forest ecosystems.

The decline of the larch forests at the southern edge of boreal forest biome from 1830 to 2016 shows spatial and temporal variations, possibly due to the warm and wet climate promoting Group B growth while reducing Group A growth. The correlation between tree growth and climate factors in principal component analysis, along with an assessment of each climate factor's contribution, lends support to this hypothesis (Fig. 4). The tree growth within our study region exhibits a pronounced sensitivity to climatic variations. The precise timing, frequency, and severity of larch forest decline are intricately tied to the spatial heterogeneity in growth-climate interactions. Specifically, the growth of *Larix gmelinii* in Group A is markedly constrained by a combination of elevated temperatures and excessively wet conditions, resulting in a higher prevalence of decline events. Nevertheless, it is noteworthy that temperature exerts a more pronounced influence on growth than precipitation, suggesting that heat stress plays a dominant role in shaping the growth trajectory of these trees.

5. Conclusions

Understanding the intricate response of boreal forests to warming trends and rising moisture levels is paramount in unraveling the underlying causes of declining forest vitality, thereby informing effective conservation and management strategies. Utilizing long-term and large-scale tree-ring width data and various climate variables, we validated assumptions about regarding the existence of forest decline on the southern edge of boreal forests. Additionally, our hierarchical clustering analysis highlights distinct differences in the timing, frequency, and severity of decline between Groups A and B. The primary impetus behind the diminished radial growth increments observed in *Larix gmelinii* was the confluence of differential response to escalating temperatures and wetter climatic conditions across varying stand densities. Our study proposes that reducing stand density is a beneficial strategy in regions with pronounced warm and wet conditions, while enhancing stand density could potentially mitigate and avert growth decline in colder and drier regions. Adjusting stand structure emerges as a vital treatment for shaping forest health and resilience. Consequently, a profound understanding of the intricate interplay between forest structure and environmental factors holds the key to mitigating adverse effects on the functionality of forest ecosystems.

CRediT authorship contribution statement

Bingqian Zhao: Writing – original draft, Data curation. **Yihong Zhu:** Writing – review & editing, Software. **Lushuang Gao:** Writing – review & editing, Project administration, Data curation. **Qibing Zhang:** Writing – review & editing. **Mingqian Liu:** Methodology. **Klaus von Gadow:** Writing – review & editing.

Human and animal rights and informed consent

This article does not contain any studies with human or animal subjects performed by any of the authors.

Data availability

Data are available on request from the authors.

Funding

National Nature Science Foundation of China (No. 32371871).

Declaration of competing interests

The authors declare that they have no known competing financial

interests or personal relationships that could have appeared to influence the work reported in this paper.

Acknowledgments

Gratitude to Professor Chunyu Zhang from Beijing Forestry University for offering guiding advice on graphical representation. Appreciation to Professor Weixue Luo from Southwest University for providing ideas on model construction. Special thanks to Professor Weiguo Liu from Northwest A & F University for offering guidance on model development. Special thanks to Professor Igor Drobyshev from the Swedish University of Agricultural Sciences and Prof. Klaus von Gadow for helping to revise the article. Thank you to Senior Rongrong Pang from Beijing Forestry University for providing the distribution of suitable areas in the article. Thanks to Chi Zhang and Zhixiao Lu from Beijing Forestry University for their assistance in data calculations.

References

Allen, C.D., Macalady, A.K., Chenchouni, H., Bachelet, D., McDowell, N., Vennetier, M., Kitzberger, T., Rigling, A., Breshears, D.D., Hogg, E.H., Gonzalez, P., Fensham, R., Zhang, Z., Castro, J., Demidova, N., Lim, J.H., Allard, G., Running, S.W., Semerci, A., Cobb, N., 2010. A global overview of drought and heat-induced tree mortality reveals emerging climate change risks for forests. Forest Ecol. Manag. 259, 660–684. https://doi.org/10.1016/j.foreco.2009.09.001.

Bai, X.P., Zhang, X.L., Li, J.X., Duan, X.Y., Jin, Y.T., Chen, Z.J., 2019. Altitudinal disparity in growth of Dahurian larch (*Larix gmelinii* Rupr.) in response to recent climate change in northeast China. Sci. Total Environ. 670, 466–477. https://doi.org/10.1016/j.scitotenv.2019.03.232.

Camarero, J.J., Gazol, A., Sangüesa-Barreda, G., Cantero, A., Sánchez-Salguero, R., Sánchez-Miranda, A., Granda, E., Serra-Maluquer, X., Ibáñez, R., 2018. Forest growth responses to drought at short- and long-term scales in Spain: squeezing the stress memory from tree rings. Front. Ecol. Evol. 6. https://doi.org/10.3389/fevo.2018.00009.

Cao, J., Liu, H.Y., Zhao, B., Li, Z.S., Liang, B.Y., Shi, L., Wu, L., Cressey, E.L., Quine, T.A., 2021. High forest stand density exacerbates growth decline of conifers driven by warming but not broad-leaved trees in temperate mixed forest in northeast Asia. Sci. Total Environ. 795, 148875. https://doi.org/10.1016/j.scitotenv.2021.148875.

Chen, Z.J., Zhang, X.L., Cui, M.X., He, X.Y., Ding, W.H., Peng, J.J., 2012. Tree-ring based precipitation reconstruction for the forest–steppe ecotone in northern Inner Mongolia, China and its linkages to the Pacific Ocean variability. Glob. Planet. Change 86–87, 45–56. https://doi.org/10.1016/j.gloplacha.2012.01.009.

Collet, C., Ningre, F., Barbeito, I., Arnaud, A., Piboule, A., 2014. Response of tree growth and species coexistence to density and species evenness in a young forest plantation with two competing species. Ann. Bot. 113, 711–719. https://doi.org/10.1093/aob/mct285.

Daly, C., Halbleib, M., Smith, J.I., Gibson, W.P., Doggett, M.K., Taylor, G.H., Curtis, J., Pasteris, P.P., 2008. Physiographically sensitive mapping of climatological temperature and precipitation across the conterminous United States. Intl. J. Climatol. 28, 2031–2064. https://doi.org/10.1002/joc.1688.

de Mello, C.R., Guo, L., Yuan, C., Rodrigues, A.F., Lima, R.R., Terra, M.C.N.S., 2024. Deciphering global patterns of forest canopy rainfall interception (FCRI): a synthesis of geographical, forest species, and methodological influences. J. Environ. Manag. 358, 120879. https://doi.org/10.1016/j.jenvman.2024.120879.

del Castillo, E.M., Zang, C.S., Buras, A., Hacket-Pain, A., Esper, J., Serrano-Notivoli, R., Hartl, C., Weigel, R., Klesse, S., de Dios, V.R., Scharnweber, T., Dorado-Liñán, I., Van der Maaten-Theunissen, M., van der Maaten, E., Jump, A., Mikac, S., Banzragch, B.E., Beck, W., Cavin, L., Claessens, H., Cada, V., Cufar, K., Dulamsuren, C., Gricar, J., Gil-Pelegrín, E., Janda, P., Kazimirovic, M., Kreyling, J., Latte, N., Leuschner, C., Longares, L.A., Menzel, A., Merela, M., Motta, R., Muffler, L., Nola, P., Petritan, A.M., Petritan, I.C., Prislan, P., Rubio-Cuadrado, A., Rydval, M., Stajic, B., Svoboda, M., Toromani, E., Trotsiuk, V., Wilmking, M., Zlatanov, T., de Luis, M., 2022. Climate-change-driven growth decline of European beech forests. Commun. Biol. 5, 163. https://doi.org/10.1038/s42003-022-03107-3.

Fritts, H.C., 1966. Growth-rings of trees: their correlation with climate: patterns of ring widths in trees in semiarid sites depend on climate-controlled physiological factors. Science 154, 3752. https://doi.org/10.1126/science.154.3752.973.

Gao, S., Liang, E.Y., Liu, R.S., Babst, F., Camarero, J.J., Fl, Y.H., Piao, S.L., Rossi, S., Shen, M.G., Wang, T., Peñuelas, J., 2022. An earlier start of the thermal growing season enhances tree growth in cold humid areas but not in dry areas. Nat. Ecol. Evol. 6, 397–404. https://doi.org/10.1038/s41559-022-01668-4.

Gauthier, S., Bernier, P., Kuuluvainen, T., Shvidenko, A.Z., Schepaschenko, D.G., 2015. Boreal forest health and global change. Science 349, 819–822. https://doi.org/10.1126/science.aaa9092.

Hernández-Alonso, H., Madrigal-González, J., Silla, F., 2023. The ecological scale mediates whether trees experience drought legacies in radial growth. Forest Ecosyst. 10, 100112. https://doi.org/10.1016/j.fecs.2023.100112.

Hijmans, R.J., Cameron, S.E., Parra, J.L., Jones, P.G., Jarvis, A., 2005. Very high resolution interpolated climate surfaces for global land areas. Int. J. Climatol. 25, 1965–1978. https://doi.org/10.1002/joc.1276.

Jia, S.H., Wang, X.G., Yuan, Z.Q., Lin, F., Ye, J., Lin, G.G., Hao, Z.Q., Bagchi, R., 2020. Tree species traits affect which natural enemies drive the Janzen-Connell effect in a temperate forest. Nat. Commun. 11, 286. https://doi.org/10.1038/s41467-019-14140-y.

Kholdaenko, Y.A., Belokopytova, L.V., Zhirnova, D.F., Upadhyay, K.K., Tripathi, S.K., Koshurnikova, N.N., Sobachkin, R.S., Babushkina, E.A., Vaganov, E.A., 2022. Stand density effects on tree growth and climatic response in *Picea obovata* Ledeb. plantations. Forest Ecol. Manag. 519, 120349. https://doi.org/10.1016/j.foreco.2022.120349.

Li, W.Q., Jiang, Y., Dong, M.Y., Du, E.Z., Zhou, Z.J., Zhao, S.D., Xu, H., 2020. Diverse responses of radial growth to climate across the southern part of the Asian boreal forests in northeast China. Forest Ecol. Manag. 458, 117759. https://doi.org/10.1016/j.foreco.2019.117759.

Li, W.Q., Manzanedo, R.D., Jiang, Y., Ma, W.Q., Du, E.Z., Zhao, S.D., Rademacher, T., Dong, M.Y., Xu, H., Kang, X.Y., Wang, J., Wu, F., Cui, X.F., Pederson, N., 2023. Reassessment of growth-climate relations indicates the potential for decline across Eurasian boreal larch forests. Nat. Commun. 14, 3358. https://doi.org/10.1038/s41467-023-39057-5.

Liu, H.Y., Williams, A.P., Allen, C.D., Guo, D.L., Wu, X.C., Anenkhonov, O.A., Liang, E.Y., Sandanov, D.V., Yin, Y., Qi, Z.H., Badmaeva, N.K., 2013. Rapid warming accelerates tree growth decline in semi-arid forests of Inner Asia. Glob. Change Biol. 19, 2500–2510. https://doi.org/10.1111/gcb.12217.

Liu, J., Li, Z.S., Keyimu, M., Wang, X.C., Liang, H.B., Feng, X.M., Gao, G.Y., Fu, B.J., 2022. Accelerated warming in the late 20th century promoted tree radial growth in the Northern Hemisphere. J. Plant Ecol. 16 (1). https://doi.org/10.1093/jpe/rtac077.

Liu, G.C., Wang, H., Yan, G.Y., Wang, M., Jiang, S., Wang, X.C., Xue, J.S., Xu, M., Xing, Y.J., Wang, Q.G., 2023. Soil enzyme activities and microbial nutrient limitation during the secondary succession of boreal forests. Catena 230, 107268. https://doi.org/10.1016/j.catena.2023.107268.

Lloyd, A.H., Bunn, A.G., 2007. Responses of the circumpolar boreal forest to 20th century climate variability. Environ. Res. Lett. 2, 045013. https://doi.org/10.1088/1748-9326/2/4/045013.

Martinez del Castillo, E., Zang, C.S., Buras, A., Hacket-Pain, A., Esper, J., Serrano-Notivoli, R., Hartl, C., Weigel, R., Klesse, S., Resco de Dios, V., Scharnweber, T., Dorado-Liñán, I., van der Maaten-Theunissen, M., van der Maaten, E., Jump, A., Mikac, S., Banzragch, B.-E., Beck, W., Cavin, L., Claessens, H., Čada, V., Čufar, K., Dulamsuren, C., Gričar, J., Gil-Pelegrín, E., Janda, P., Kazimirovic, M., Kreyling, J., Latte, N., Leuschner, C., Longares, L.A., Menzel, A., Merela, M., Motta, R., Muffler, L., Nola, P., Petritan, A.M., Petritan, I.C., Prislan, P., Rubio-Cuadrado, Á., Rydval, M., Stajić, B., Svoboda, M., Toromani, E., Trotsiuk, V., Wilmking, M., Zlatanov, T., de Luis, M., 2022. Climate-change-driven growth decline of European beech forests. Commun. Biol. 5 (1). https://doi.org/10.1038/s42003-022-03107-3.

Murtagh, F., Legendre, P., 2014. Ward's hierarchical agglomerative clustering method: which algorithms implement ward's criterion? J. Classif. 31, 274–295. https://doi.org/10.1007/s00357-014-9161-z.

Nowacki, G.J., Abrams, M.D., 1997. Radial-growth averaging criteria for reconstructing disturbance histories from presettlement-origin oaks. Ecol. Monogr. 67, 225–249. https://doi.org/10.1890/0012-9615(1997)067[0225:RGACFR]2.0.CO;2.

Pang, R., Zhao, B., 2023. Relationship between climatic suitability and productivity of *Larix gmelinii* forest. J. Beijing For. Univ. 45, 1–10. https://doi.org/10.12171/j.10001522.20220361.

Podlaski, R., 2021. Variability in radial increment can predict an abrupt decrease in tree growth during forest decline: tree-ring patterns of *Abies alba* Mill. in near-natural forests. Forest Ecol. Manag. 479, 118579. https://doi.org/10.1016/j.foreco.2020.118579.

Reineke, L.H., 1993. Perfecting a stand-density index for even-aged forests. J. Agric. Res. 46, 627–638.

Sánchez-Salguero, R., Camarero, J.J., Gutiérrez, E., Rouco, F.G., Gazol, A., Sanguesa-Barreda, G., Andreu-Hayles, L., Linares, J.C., Seftigen, K., 2017. Assessing forest vulnerability to climate warming using a process-based model of tree growth: bad prospects for rear-edges. Glob. Change Biol. 23, 2705–2719. https://doi.org/10.1111/gcb.13541.

Wang, C., Gower, S.T., Wang, Y., Zhao, H.X., Yan, P., Bond-Lamberty, B.P., 2001. The influence of fire on carbon distribution and net primary production of boreal *Larix gmelinii* forests in north-eastern China. Glob. Change Biol. 7, 719–730. https://doi.org/10.1046/j.1354-1013.2001.00441.x.

Wang, T.L., Wang, G.Y., Innes, J.L., Seely, B., Chen, B.Z., 2017. ClimateAP: an application for dynamic local downscaling of historical and future climate data in Asia Pacific. Front. Agr. Sci. Eng. 4, 448. https://doi.org/10.15302/J-FASE-2017172.

Wang, Y.B., Liu, X.H., Anhäuser, T., Lu, Q.Q., Zeng, X.M., Zhang, Q.L., Wang, K.Y., Zhang, L.N., Zhang, Y., Keppler, F., 2020. Temperature signal recorded in δ^2H and $\delta^{13}C$ values of wood lignin methoxyl groups from a permafrost forest in northeastern China. Sci. Total Environ. 727, 138558. https://doi.org/10.1016/j.scitotenv.2020.138558.

Wang, X., Xu, K., Miao, W., Gao, L., Ullah, S., Lyu, Y., Wang, X., 2022. Functional traits and stand factors as strong drivers of radial growth response to hotter drought in a temperate forest of North China. Eur. J. Forest Res. 141, 927–938. https://doi.org/10.1007/s10342-022-01482-4.

Wei, X., Liang, W., 2021. Regulation of stand density alters forest structure and soil moisture during afforestation with *Robinia pseudoacacia* L. and *Pinus tabulaeformis* Carr. on the Loess Plateau. Forest Ecol. Manag. 491, 119196. https://doi.org/10.1016/j.foreco.2021.119196.

Yang, H., Ciais, P., Frappart, F., Li, X.J., Brandt, M., Fensholt, R., Fan, L., Saatchi, S., Besnard, S., Deng, Z., Bowring, S., Wigneron, J.P., 2023. Global increase in biomass carbon stock dominated by growth of northern young forests over past decade. Nat. Geosci. 16, 886–892. https://doi.org/10.1038/s41561-023-01274-4.

Yasmeen, S., Wang, X., Zhao, H., Zhu, L.J., Yuan, D.Y., Li, Z.S., Zhang, Y.D., Ahmad, S., Han, S.J., 2019. Contrasting climate-growth relationship between *Larix gmelinii* and *Pinus sylvestris* var. *mongolica* along a latitudinal gradient in Daxing'an Mountains, China. Dendrochronologia 58, 125645. https://doi.org/10.1016/j.dendro.2019.125645.

Yu, J., Shah, S., Zhou, G., Xu, Z.Z., Liu, Q.J., 2018. Tree-ring-recorded drought variability in the Northern Daxing'anling mountains of Northeastern China. Forests 9, 674. https://doi.org/10.3390/f9110674.

Zhang, X., 2022. Radial Growth Characteristics of *Larix Gmelinii* in Genhe Inner Monglia and its Response to Climate Factors. Master Thesis, Inner Mongolia Agricultural University,. China.

Zhang, Q., Lv, X., Yu, X., Ni, Y., Ma, L., Liu, Z.Q., 2022a. Species and spatial differences in vegetation rainfall interception capacity: a synthesis and meta-analysis in China. Catena 213, 106223. https://doi.org/10.1016/j.catena.2022.106223.

Zhang, X., Yu, P., Wang, D., Xu, Z., 2022b. Density- and age- dependent influences of droughts and intrinsic water use efficiency on growth in temperate plantations. Agric. Forest Meteorol. 325, 109134. https://doi.org/10.1016/j.agrformet.2022.109134.

Zhang, X., Shu, C., Wu, Y., Ye, P., Du, D.W., 2023. Advances of coupled water-heat-salt theory and test techniques for soils in cold and arid regions: a review. Geoderma 432, 116378. https://doi.org/10.1016/j.geoderma.2023.116378.

Zheng, P.F., Wang, D.D., Jia, G.D., Yu, X.X., Liu, Z.Q., Wang, Y.S., Zhang, Y.G., 2022a. Variation in water supply leads to different responses of tree growth to warming. Forest Ecosyst 9, 100003. https://doi.org/10.1016/j.fecs.2022.100003.

Zheng, X., An, Z., Cao, M., Wu, F., Guan, X., Chang, S.X., Liu, S.L., Jiang, J., 2022b. Arbuscular mycorrhizal hyphal respiration makes a large contribution to soil respiration in a subtropical forest under various N input rates. Sci. Total Environ. 852, 158309. https://doi.org/10.1016/j.scitotenv.2022.158309.

Zhou, H., Chen, Y., Zhu, C., Zhu, C.G., Li, Z., Fang, G.H., Li, Y.P., Fu, A.H., 2020. Climate change may accelerate the decline of desert riparian forest in the lower Tarim River, Northwestern China: evidence from tree-rings of *Populus euphratica*. Ecol. Ind. 111, 105997. https://doi.org/10.1016/j.ecolind.2019.105997.